Modulation of L-Type Ca^{2+} Current by Fast and Slow Ca^{2+} Buffering in Guinea Pig Ventricular Cardiomyocytes

Yongdong You, Dieter J. Pelzer, and Siegried Pelzer
Membrane Transport and Signaling Group, Department of Physiology and Biophysics, Dalhousie University, Halifax, Nova Scotia B3H 4H7, Canada

ABSTRACT Free Ca^{2+} near Ca^{2+} channel pores is expected to be lower in cardiomyocytes dialyzed with bis-(o-amino-phenoxy)-ethane-N,N,N',N'-tetraacetic acid (BAPTA) than with ethyleneglycol-bis-(β-aminoethyl)-N,N,N',N'-tetraacetic acid (EGTA) because BAPTA chelates incoming Ca^{2+} more rapidly. The consequences of intracellular Ca^{2+} buffering by BAPTA (0.2–60 mM) and by EGTA (0.2–67 mM) on whole-cell L-type Ca^{2+} current ($I_{Ca,L}$) were investigated in voltage-clamped guinea pig ventricular cardiomyocytes; bulk cytoplasmic free Ca^{2+} (Ca_c^{2+}) was monitored using the fluorescent Ca^{2+} indicator indo-1. $I_{Ca,L}$ was augmented by ~12-fold when BAPTA in the cell dialysate was increased from 0.2 to 50 mM (half-maximal stimulation at 31 mM), whereas elevating internal EGTA from 0.2 to 67 mM increased $I_{Ca,L}$ only by ~2-fold. Ca_c^{2+} was <20 nM with internal BAPTA or EGTA $\geq$ 20 mM. While EGTA up to 67 mM had only an insignificant inhibitory effect on the stimulation of $I_{Ca,L}$ by 3 μM forskolin, $I_{Ca,L}$ in 50 mM BAPTA-dialyzed myocytes was insensitive to forskolin-induced elevation of adenosine 3',5'-cyclic monophosphate (cAMP); conversely, $I_{Ca,L}$ in cAMP-loaded cells was unresponsive to BAPTA dialysis. Cell dialysis with BAPTA, but not with EGTA, accelerated the slow component of $I_{Ca,L}$ inactivation (τ_S) without affecting its fast component (τ_F), resembling the effects of cAMP-dependent phosphorylation. BAPTA-stimulated $I_{Ca,L}$ was inhibited by acetylcholine and by the cAMP-dependent protein kinase (PKA) blocker H-89. These results suggest that BAPTA-induced lowering of peri-channel Ca^{2+} stimulates cAMP synthesis and channel phosphorylation by disinhibiting Ca^{2+}-sensitive adenylyl cyclase.

INTRODUCTION

Intracellular Ca^{2+} (Ca_i^{2+}) modulates both magnitude and duration of Ca^{2+} entry through L-type Ca^{2+} channels ($I_{Ca,L}$), thus providing an intrinsic feedback mechanism for Ca^{2+} homeostasis in heart. Both stimulation and inhibition of $I_{Ca,L}$ by elevation of Ca_i^{2+} have been observed depending on experimental conditions (You et al., 1994; see McDonald et al., 1994 for review). In regard to stimulation, this putative positive feedback mechanism seems to involve a Ca_i^{2+}-dependent enzymatic pathway that ends in phosphorylation of L-type Ca^{2+} channels by enhanced PKA and/or other kinase activity (Gurney et al., 1989; Hadley and Lederer, 1991; Hirano and Hiraoka, 1994; You et al., 1994; see McDonald et al., 1994 for review). Concerning inhibition, elevation of Ca_i^{2+} by (i) cell dialysis with high Ca^{2+} solutions (Kokubun and Irisawa, 1984; Tseng and Boyden, 1991), (ii) lowering external Na^+ (which compromises Ca^{2+} extrusion via the Na^+-Ca^{2+} exchanger, cf. You et al., 1994), (iii) increasing external Ca^{2+} during K^+ depolarization (Hirano and Hiraoka, 1994), and (iv) flashphotolysis of caged Ca^{2+} (Hadley and Lederer, 1991) can switch on a fast powerful $I_{Ca,L}$ inactivation process that is superimposed on a slower voltage-dependent mechanism (e.g., McDonald et

al., 1994). In regard to the mechanism underlying Ca_i^{2+} inhibition of $I_{Ca,L}$, we have recently proposed two distinct cytoplasmic inactivation sites at the channel protein, one of which directly interacts with submembrane free Ca^{2+} in the vicinity of the Ca^{2+} channel pore (Ca_{sm}^{2+}), whereas the other is regulated by a yet unknown mediator activated by bulk cytosolic free Ca^{2+} (Ca_c^{2+}; You et al., 1995). This model raises the possibility of differential roles of Ca_c^{2+} and Ca_{sm}^{2+} in the feedback modulation of $I_{Ca,L}$. However, such a possibility has not been explored in previous studies, in which Ca_c^{2+} and Ca_{sm}^{2+} were generally referred to as intracellular free Ca^{2+}, or Ca_i^{2+}.

The free Ca^{2+} at each point in space within the cytoplasm is determined by the balance between the supply of Ca^{2+} to this point and diffusion of Ca^{2+} away from the point as well as by Ca^{2+} sequestration. Thus, due to the limited diffusion rate of Ca^{2+}, as well as the slow rate of Ca^{2+} sequestration, high Ca^{2+} concentrations can theoretically develop underneath the plasma membrane as the result of Ca^{2+} entry through membrane Ca^{2+} channels (Neher, 1986; Kargacin and Fay, 1991; Stern, 1992, Kargacin, 1994). Local Ca^{2+} signaling in this submembrane space (e.g., Lederer et al., 1990; Leblanc and Hume, 1990 for cardiac muscle; Smith and Augustine, 1988 for neurons) may, for example, facilitate the coupling of Ca^{2+} entry to Ca^{2+} release and/or locally activate specific signal transduction pathways, before, or without activating other Ca^{2+}-dependent pathways in the central cytoplasm of the cell (cf. Kargacin, 1994). The latter possibility has gained particular attention by recent findings which suggest that local Ca^{2+} signals can regulate adenylyl cyclase activity in a variety of cells (cf. Cooper et

al., 1995; Sunahara et al., 1996). In chick cardiac cells and membranes, for example, Ca^{2+} entry via L-type Ca^{2+} channels is suggested to act as a negative regulator of types V and VI adenylyl cyclase activities and cAMP levels (Yu et al., 1993). The evidence for this has been indirect, however, and the effects of local Ca^{2+} changes on $I_{Ca,L}$ have not been explored experimentally.

Thus, the objective of the present study was to investigate whether changes in Ca_{sm}^{2+} affect $I_{Ca,L}$ differently than changes in Ca_c^{2+}. To this end, we utilized two different Ca^{2+} chelators, EGTA and BAPTA, at different concentrations in the cell dialysates. Although, at steady-state, both chelators bind Ca^{2+} with similar affinities (apparent K_D for EGTA and BAPTA is 149 nM and 127 nM at pH 7.2, respectively), BAPTA, due to its faster Ca^{2+} binding kinetics ($K_{on} = 9.4 \times 10^8$ M^{-1} s^{-1}, Lattanzio and Bartschat, 1991), chelates incoming Ca^{2+} faster than EGTA ($K_{on} = 1.5 \times 10^6$ M^{-1} s^{-1}, Smith et al., 1984). Consequently, EGTA is ineffective in buffering Ca^{2+} within macromolecular distances of the Ca^{2+} channel pore, whereas useful Ca^{2+} buffering in this restricted diffusion space can be achieved with the faster Ca^{2+} chelator BAPTA. $I_{Ca,L}$ was measured using the whole-cell patch clamp technique; Ca_c^{2+} was determined simultaneously by ratiometric measurements of indo-1 fluorescence. Here, we report that cell dialysis with 50 mM BAPTA increased $I_{Ca,L}$ by ~12-fold as compared to $I_{Ca,L}$ in 0.2 mM BAPTA-dialyzed cells; an increase in dialysate EGTA from 0.2 to 67 mM augmented $I_{Ca,L}$ by only ~2-fold. Bulk cytoplasmic free Ca^{2+} was below 20 nM under both conditions. In contrast to EGTA-modified current, $I_{Ca,L}$ in BAPTA-dialyzed myocytes was insensitive to forskolin-induced elevation of cAMP; conversely, $I_{Ca,L}$ in cAMP-loaded myocytes was unresponsive to subsequent BAPTA dialysis. Furthermore, BAPTA-stimulated $I_{Ca,L}$ was reversibly inhibited by acetylcholine-mediated suppression of adenylyl cyclase activity and by the PKA blocker H-89. These results suggest that BAPTA-induced lowering of Ca_{sm}^{2+} in the vicinity of the Ca^{2+} channel pore increases cellular cAMP levels by disinhibiting Ca^{2+}-sensitive adenylyl cyclase, resulting in channel phosphorylation via PKA and $I_{Ca,L}$ stimulation.

METHODS

Single ventricular myocytes were enzymatically dissociated from adult guinea pig (350–650 g) hearts, as previously described (You et al., 1994). Dissociated myocytes were stored in "KB medium" (see You et al., 1994 for composition) at room temperature before experiments.

For experimental recording, isolated cells in KB medium were transferred to a superfusion chamber mounted on top of an inverted microscope stage (Olympus IMT-2, Tokyo, Japan). Once the myocytes had adhered to the glass bottom of the chamber, they were superfused with a control Tyrode solution containing (in mM) 140 NaCl, 5.4 KCl, 1.8 CaCl_2, 1.0 MgCl_2, 10 HEPES, 10 glucose (pH 7.4). After 5 min, the superfusate was changed to K^+-free Tyrode (KCl replaced by CsCl). After giga-seal formation and patch breakthrough, voltage clamp was applied with an EPC-9 patch-clamp amplifier (HEKA, Lambrecht/Pfalz, Germany; pipette resistance 1.5–3 MΩ when immersed in control Tyrode) using the whole-cell configuration of the patch-clamp technique (Hamill et al., 1981). $I_{Ca,L}$

was elicited by 100-ms step depolarization to 0 mV from a holding potential of −40 mV at 0.08 Hz. Currents and voltages were recorded on Atari Megafile 44 disks and analyzed on an Atari Mega 4 computer (Atari Data Analysis software 3.11, Instrutech Corp., Elmont, NY). $I_{Ca,L}$ is expressed as current density (in pA/pF); cell capacitance (90–210 pF) was automatically updated with each current recording.

Myocytes were dialyzed through the electrode opening (access resistance 2–7 MΩ) with intracellular solutions containing 0.2–67 mM Ca^{2+} chelators (EGTA, Aldrich, Milwaukee, WI or BAPTA, Sigma, St. Louis, MO). Three stock intracellular solutions (IS-0, IS-E, and IS-B) were prepared and stored at −20°C. IS-0 was Ca^{2+} buffer-free and contained (in mM) 50 CsCl, 110 cesium aspartate, 10 HEPES, 2 MgCl_2, 4 MgATP (pH 7.2). In IS-E and IS-B, 67 mM EGTA and 67 mM BAPTA, respectively, were added, with cesium aspartate reduced to 11 mM to balance the osmolarity. IS-E and IS-B were proportionally mixed with IS-0 before an experiment to obtain the desired final concentrations of Ca^{2+} buffers in the cell dialysate. The intracellular solution containing 5,5'-dinitro-BAPTA (dn-BAPTA) (Molecular Probes, Eugene, OR) was prepared separately and contained (in mM) 50 CsCl, 60 cesium aspartate, 10 HEPES, 2 MgCl_2, 4 MgATP, 20 BAPTA, 20 dn-BAPTA (pH 7.2). Forskolin (3 µM, Sigma), IBMX (50 µM, Sigma) and H-89 dihydrochloride (100 µM, Calbiochem, La Jolla, CA) were diluted in K^+-free Tyrode before experiments from 10 to 50 mM stock solutions prepared in DMSO. Acetylcholine (10 µM, Sigma) solution was prepared from a 10-mM aqueous stock. In experiments using ryanodine (Sigma), 1 mM aqueous solution was freshly prepared and mixed with the cell suspension at a final concentration of 10 µM. Cells were incubated with ryanodine at room temperature for 0.5–5 h, transferred to the recording chamber, and superfused with the K^+-free Tyrode, also containing 10 µM ryanodine. To achieve maximal cAMP loading before electrophysiological recording, cells were preincubated with 3 µM forskolin and 50 µM IBMX for 20–50 min at room temperature.

In experiments where intracellular Ca^{2+} (Ca_c^{2+}) was monitored, 50 µM indo-1 (pentapotassium salt, Molecular Probes) was added to the cell dialysate from a 1 mM aqueous stock. A PTI Deltascan-4000 ratio-fluorescence system (Photon Technology International, South Brunswick, NJ) was used to measure indo-1 fluorescence. The excitation was set at 355 nm by a monochromator (band pass 3 nm), and the emission was split by a dichroic cube assembly, comprising a dichroic mirror (455 nm) and two bandpass filters (405/10 nm and 485/10 nm). The ratio of emission fluorescence at 405 and 485 nm, after background correction, was converted to Ca_c^{2+} according to Grynkiewicz et al. (1985)

$$Ca_c^{2+} = K_D\beta \, (R - R_{min})/(R_{max} - R),$$

where K_D (392 nM), β (1.934), R_{max} (1.296), and R_{min} (0.147) were determined as previously described (You et al., 1994). Ca_c^{2+} below 5% of K_D (~20 nM) can not be determined with certainty. In such cases, a Ca_c^{2+} < 20 nM was given. All experiments were performed at 22 ± 1°C.

Results in this study were expressed as means ± SEM. Statistic comparisons were made using Student's t-test. $p < 0.05$ was considered statistically significant.

RESULTS

The experimental results are presented under three subheadings. We will start with a description of $I_{Ca,L}$ augmentation by cell dialysis with high concentrations of BAPTA as compared to high EGTA dialysis. Secondly, we will assess the Ca^{2+} buffering characteristics of BAPTA, in comparison to EGTA, at different points in space of the cytoplasm, and provide evidence bridging the stimulatory action of BAPTA on $I_{Ca,L}$ and the superior Ca^{2+} buffering by BAPTA within macromolecular distances of the Ca^{2+} channel pore. Finally, we will present data that strongly suggest the involvement of increased adenylyl cyclase activity,

cAMP synthesis, and PKA-dependent phosphorylation in the BAPTA-induced augmentation of $I_{Ca,L}$.

Effects of cell dialysis with various concentrations of EGTA and BAPTA on $I_{Ca,L}$

A common observation during whole-cell recording of $I_{Ca,L}$ using the patch-clamp technique is the decline of $I_{Ca,L}$ amplitude with time. This phenomenon is known as current rundown, which is likely caused by a combination of many factors resulting from the change in the intracellular environment during cell dialysis (cf. McDonald et al., 1994). Fig. 1 A illustrates a typical example of $I_{Ca,L}$ rundown in a myocyte dialyzed with a 40 mM EGTA-containing solution. Fast $I_{Ca,L}$ rundown occurred in the first 300 s after patch breakthrough, which accounted for 70% of the total rundown. This was followed by a slower phase, which ac-
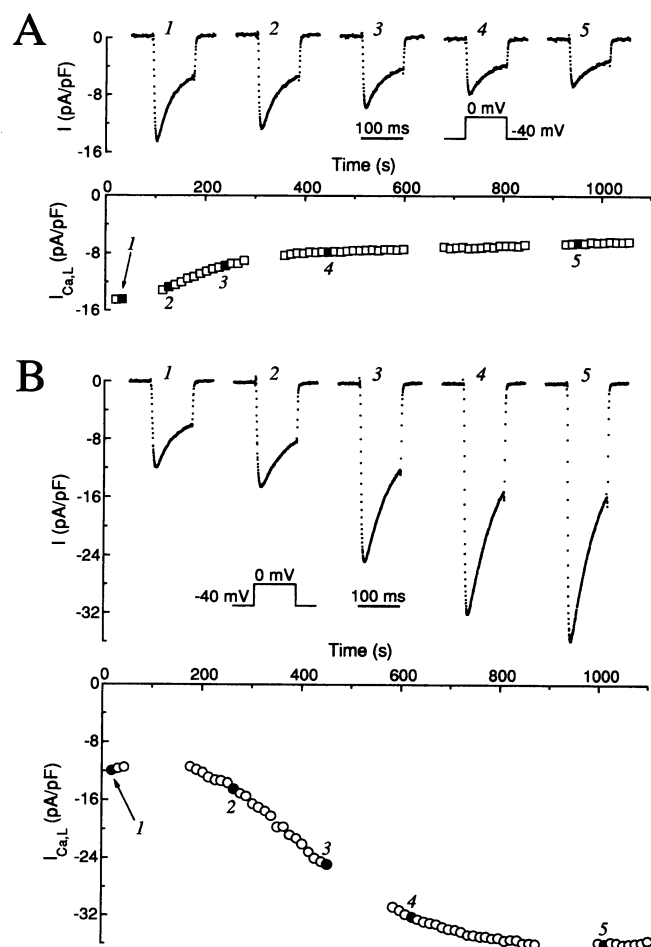

FIGURE 1   Comparison of $I_{Ca,L}$ time courses in guinea pig ventricular cardiomyocytes dialyzed with a 40-mM EGTA-containing solution (A) and a 40-mM BAPTA-containing solution (B), respectively. In both time course illustrations, "0" time represents the moment of patch breakthrough and the start of cell dialysis. Filled symbols (1 to 5) in each time course correspond to sample currents shown in the panels above. Breaks in the time courses indicate times when the current-voltage (I-V) relations were determined (cf. Fig. 2 A).

counted for the remaining 30% of the rundown. Fig. 1 B shows a very different time course of $I_{Ca,L}$ in a myocyte during dialysis with a 40 mM BAPTA-containing solution. In ~200 s, the initial rundown was overcome by a progressive augmentation of $I_{Ca,L}$ with time (i.e., a "run-up"). At >800 s, peak $I_{Ca,L}$ in the BAPTA-dialyzed myocyte was ~5× larger than peak $I_{Ca,L}$ recorded in the EGTA-dialyzed cell (compare sample currents 5 in Fig. 1, A and B). This novel change of $I_{Ca,L}$ during intracellular dialysis with 40 mM BAPTA was observed in all 17 cells studied (also see Fig. 4 for a summary).

The experiments summarized in Fig. 2 were designed to examine whether the 40 mM BAPTA-augmented inward current preserved all the characteristics of $I_{Ca,L}$. Fig. 2 Aa shows example currents elicited from a holding potential of −40 mV to 5 test potentials ranging from −20 to +30 mV, measured shortly (40–180 s) after patch breakthrough (Control), and after >800 s dialysis with 40 mM EGTA (EGTA) or 40 mM BAPTA (BAPTA). Fig. 2 Ab illustrates the relationships between peak $I_{Ca,L}$ and test potential (I-V) over a −30 to +80 mV voltage range. Prolonged cell dialysis with 40 mM EGTA solution reduced $I_{Ca,L}$ over the entire potential range (Fig. 2 Aa, EGTA; Fig. 2 Ab, triangles). In the late stage of 40-mM BAPTA dialysis, $I_{Ca,L}$ was often large enough (especially in myocytes >150 pF) to result in loss of voltage control ~ −10 mV. In smaller cells, however, borderline voltage control seems to be maintained in this critical potential range (e.g., Fig. 2 Aa, BAPTA; Fig. 2 Ab, circles). The original records (Fig. 2 Aa, BAPTA) as well as the I-V relation (Fig. 2 Ab, circles) from one of these myocytes after prolonged 40-mM BAPTA dialysis suggest that $I_{Ca,L}$ was enhanced over the entire potential range examined. Typical bell-shaped $I_{Ca,L}$-V relations were observed in myocytes before extensive internal solution exchange (squares) and after dialysis with either 40 mM EGTA (triangles) or 40 mM BAPTA (circles). It is also worth noting that cell dialysis with EGTA and BAPTA seemingly resulted in small positive and negative shifts of the potential eliciting maximum inward current (V_{max}), respectively (Fig. 2 Ab), as revealed by Spline approximations of the I-V relations (Origin 4.0, Microcal Software Inc., Northampton, MA). Fig. 2 B shows that extracellular application of 0.2 mM Cd^{2+}, a specific blocker of L-type Ca^{2+} channels, reversibly inhibited BAPTA-enhanced inward current by 95.2 ± 0.3% ($n = 5, p < 0.0001$). Finally, since the BAPTA-stimulated inward current is comparable in size to the large Na^+ current flowing through Ca^{2+} channel ($I_{Ca(Na),L}$) in the virtual absence of external Ca^{2+} (cf. McDonald et al., 1994), we explored the possibility that high BAPTA reverses the ionic selectivity of the Ca^{2+} channel, thus allowing Na^+ influx even in the presence of 1.8 mM external Ca^{2+}. The experiment illustrated in Fig. 2 C reveals that BAPTA-stimulated current was not significantly reduced ($n = 5, p = 0.82$) upon complete substitution of external Na^+ with equimolar TEA^+, a rather poor channel permeant. This argues directly against the Na^+ permeation hypothesis.

FIGURE 2 Characteristics of BAPTA-stimulated inward current. Panel *Aa* illustrates original current records elicited from holding potential -40 mV to test potentials ranging from -20 to $+30$ mV (*1*, -20 mV; *2*, -10 mV; *3*, 0 mV; *4*, $+10$ mV; *5*, $+30$ mV) before (*Control*) and after cell dialysis with either 40 mM EGTA solution (*EGTA*) or 40 mM BAPTA solution (*BAPTA*). Panel *Ab* compares *I-V* relations from -30 to $+80$ mV test potentials obtained under the above three conditions (*squares*, Control; *triangles*, EGTA; *circles*, BAPTA). Panel *B* illustrates the effect of bath application of 0.2 mM Cd^{2+} on BAPTA-enhanced inward current. A representative time course and sample currents are shown in the left and center panels, respectively (*Ba*); the average amplitudes of BAPTA-stimulated current before (*Ctrl*) and after (*Cd^{2+}*) the application of Cd^{2+} are summarized in *Bb* ($n = 5$). Panel *C* shows the effect of external Na^+ substitution with tetraethylammonium (*TEA^+*) on BAPTA-enhanced inward current. Shown in *Ca* are a typical time course and sample currents. The amplitudes of the inward current before (*Ctrl*) and after TEA^+ substitution (*TEA^+*) are summarized in *Cb* ($n = 5$).
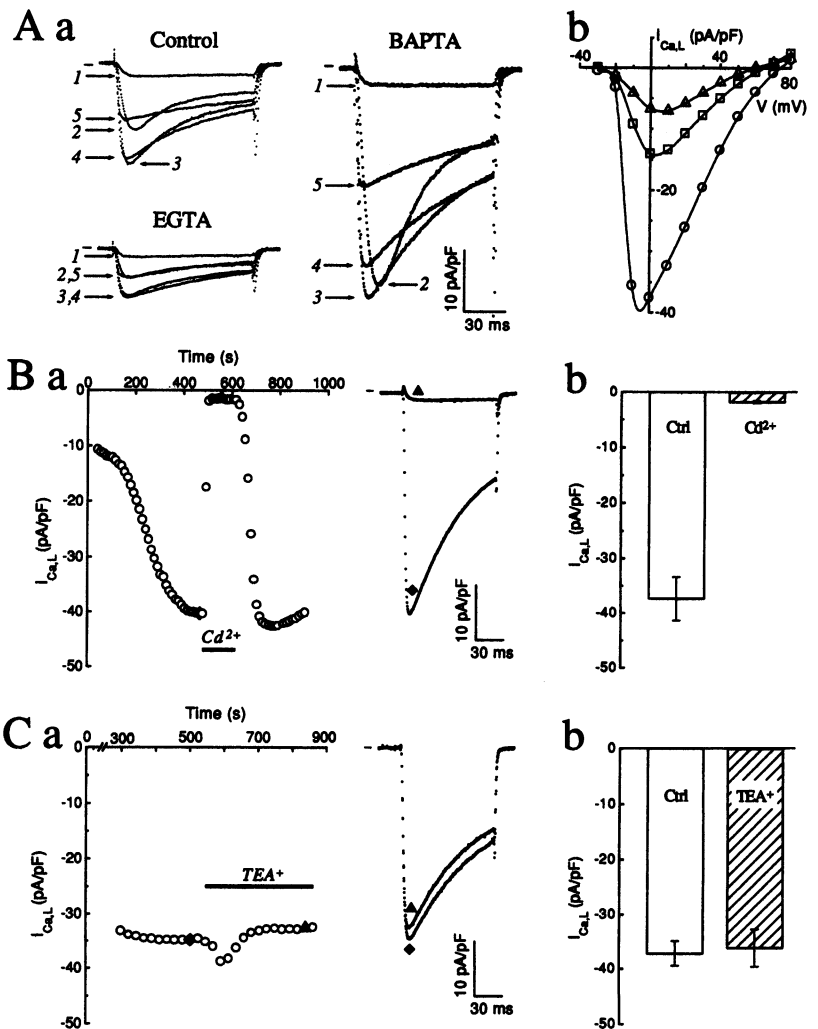
Fig. 3 shows the time courses of $I_{Ca,L}$ recorded in myocytes dialyzed with three different concentrations of EGTA and BAPTA, respectively. When the EGTA concentration was increased in the cell dialysate, the slow phase of $I_{Ca,L}$ rundown was retarded in a concentration-dependent manner, thus allowing a progressively larger $I_{Ca,L}$ to flow after prolonged dialysis with higher EGTA concentrations (Fig. 3 *A*). When 0.2 mM BAPTA was included in the cell dialysate, no augmentation of $I_{Ca,L}$ was observed; a rundown of $I_{Ca,L}$ similar to that with 0.2 mM EGTA was observed (Fig. 3 *Ba*). Run-up of $I_{Ca,L}$ became evident when the dialysate BAPTA concentration was increased to 30 mM, and it was much more pronounced during 40-mM BAPTA dialysis (Fig. 3 *Ba*). Compared to the 40-mM BAPTA time course, the $I_{Ca,L}$ increment with 30 mM BAPTA in the internal solution was smaller and took more time to develop (i.e., longer $t_{1/2}$). Fig. 3 *Bb* shows that among cells dialyzed with 40 mM BAPTA, the half time for maximal $I_{Ca,L}$ stimulation ($t_{1/2}$) was inversely related to the rate of BAPTA dialysis into the cells: faster cell dialysis (smaller cell and/or lower access resistance) corresponded to shorter $t_{1/2}$, and vice

versa. Such quantitative evidence strongly suggests a direct correlation between the accumulation of BAPTA in the cytoplasm and the stimulation of $I_{Ca,L}$.

Fig. 4 summarizes the dependence of $I_{Ca,L}$ on the Ca^{2+} chelator concentrations in the cell dialysates. For cells dialyzed with ≥ 30 mM BAPTA, $I_{Ca,L}$ values were obtained after maximal effects of BAPTA dialysis were reached. $I_{Ca,L}$ values from the rest of cells (where no net run-up was observed) were obtained at comparable times after patch breakthrough. When EGTA was used as a Ca^{2+} chelator (*triangles*), a near doubling of $I_{Ca,L}$ was observed when its concentration was increased from 0.2 to 67 mM. In contrast, a much larger $I_{Ca,L}$-enhancing effect of BAPTA (*circles*) developed steeply at concentrations >20 mM. At 50 mM BAPTA, $I_{Ca,L}$ was 12.3-fold larger than at 0.2 mM. The BAPTA concentration at which half-maximal stimulation of $I_{Ca,L}$ occurred was derived from the sigmoidal fit to the data and was determined to be 31 mM. This significantly larger enhancement of $I_{Ca,L}$ by BAPTA may suggest a distinct underlying cellular mechanism, which will be the subject of our investigation in the remainder of this study.
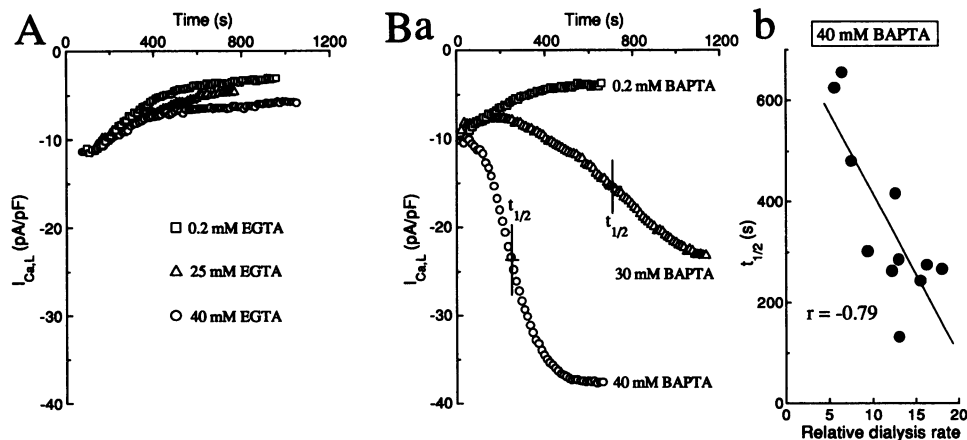
FIGURE 3   Dependence of $I_{Ca,L}$ time courses on internal EGTA (A) and BAPTA concentration (Ba) and on the rate of cell dialysis (Bb). (A) time courses of $I_{Ca,L}$ in three myocytes dialyzed with 0.2 mM, 25 mM, and 40 mM EGTA, respectively. (Ba), time courses of $I_{Ca,L}$ in three myocytes dialyzed with 0.2 mM, 30 mM, and 40 mM BAPTA, respectively. $t_{1/2}$ corresponds to half-maximal stimulation of $I_{Ca,L}$ during cell dialysis of 30 mM and 40 mM BAPTA. (Bb) correlation between $t_{1/2}$ and the rate of cell dialysis ($\alpha R_A^{-1} C_M^{-1.5}$, where R_A and C_M are access resistance and cell capacitance, respectively; Pusch and Neher, 1988) in 10 cells dialyzed with 40 mM BAPTA solution. The straight line is a linear fit of all data points. r = correlation coefficient.

Buffering of Ca_c^{2+} and Ca_{sm}^{2+} by intracellular EGTA and BAPTA

Fig. 5 shows the behavior of $I_{Ca,L}$ simultaneously with Ca_i^{2+}, when guinea pig ventricular cardiomyocytes were dialyzed with solutions containing low and high concentrations of EGTA and BAPTA, respectively. Because the microfluorometric method used collects indo-1 fluorescence over a large area of a myocyte, the measured intracellular free Ca^{2+} level represents an average Ca_i^{2+}, which closely reflects bulk cytosolic free Ca^{2+}, Ca_c^{2+}. With both 0.2 and 40 mM internal EGTA (Fig. 5 A, a and b, respectively), $I_{Ca,L}$ progressively decreased with time. At comparable times after patch breakthrough, $I_{Ca,L}$ densities with 0.2 mM EGTA were ~50% of those with 40 mM EGTA; average Ca_c^{2+} values were 93.7 ± 9.2 nM (n = 4) and <20 nM (n = 7), respectively. Equimolar substitution of 0.2 mM EGTA with BAPTA (Fig. 5 Ba) did not significantly alter $I_{Ca,L}$ run-down or Ca_c^{2+} level (82.9 ± 6.4 nM, n = 7). However, when intracellular BAPTA was increased to 40 mM, there was a progressive rise in $I_{Ca,L}$ density that plateaued at ~11 times the density recorded with 0.2 mM BAPTA dialysate (Fig. 5 Bb). Despite this large increase in Ca^{2+} influx, Ca_c^{2+} remained < 20 nM.

Fig. 6 A illustrates Ca_c^{2+} changes in myocytes dialyzed with 0.2–40 mM of either Ca^{2+} chelator. As shown in Fig. 6 Aa, Ca_c^{2+} was 92 nM in quiescent myocytes held at −40 mV and dialyzed with 0.2 mM BAPTA. Membrane depolarizations to 0 mV for 100 ms induced transient elevations of Ca_c^{2+}. Cell dialysis with either 40 mM EGTA or 40 mM BAPTA reduced the resting Ca_c^{2+} to <20 nM (which is considered the detection limit of indo-1, see Methods for details) and completely suppressed the depolarization-triggered Ca_c^{2+} transients. Fig. 6 Ab summarizes the dependence of the indo-1 fluorescence ratio on intracellular Ca^{2+}

chelator concentration. It is evident that at concentrations >20 mM, both EGTA and BAPTA are equally effective in reducing Ca_c^{2+} to a minimal level.

The present microfluorometry does not provide enough spatial resolution to detect Ca^{2+} concentration gradients between different points in space within the cytoplasm. In Fig. 6 B, we employed a mathematical model developed by Stern (1992) to calculate the Ca^{2+} concentration gradient as a function of the distance from the Ca^{2+} channel pore in the presence of EGTA ($top\ panel$) and BAPTA ($bottom\ panel$), respectively. This model was designed to calculate steady-state Ca_{sm}^{2+} profiles in the vicinity of a single Ca^{2+} channel pore, conducting picoampere elementary Ca^{2+} current $i_{Ca,L}$. To adapt this model to a whole-cell setting, we made two different assumptions regarding $i_{Ca,L}$ to account for the changes in $I_{Ca,L}$ after cell dialysis with EGTA or BAPTA (see Discussion for rationale). (i) $i_{Ca,L}$ was assumed to change proportionally with $I_{Ca,L}$ (Fig. 6 B, $left\ panels$), although we realize that any change of Ca^{2+} entry at the single-channel level is likely to be mediated by changes in channel open probability and/or availability. Unfortunately, the latter option is not available in the present model. (ii) $i_{Ca,L}$ was independent of peak $I_{Ca,L}$ (Fig. 6 B, $right\ panels$). Regardless of either assumption, these calculations show qualitatively that the effective degree of buffering near the pore is markedly affected by the kinetics of the Ca^{2+} buffer. EGTA solutions are relatively ineffective in buffering Ca^{2+} within macromolecular distances of the pore (20–100 nm), while they buffer Ca^{2+} well toward the center of the cytoplasm (say, at 500 nm away from the pore; Fig. 6 Ba). With the fast buffer BAPTA at higher concentrations (Fig. 6 Bb), Ca^{2+} declines much faster in the vicinity of the Ca^{2+} channel pore. For example, at a distance of 30 nm from the pore, Ca_{sm}^{2+} is 0.02–0.2 μM with 40 mM BAPTA, while it
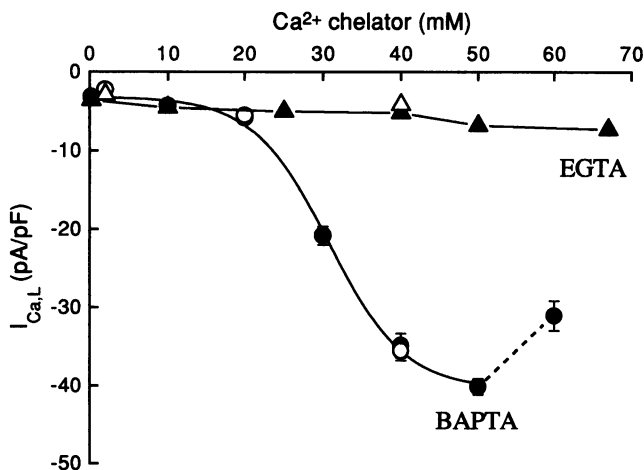
FIGURE 4 Concentration dependence of $I_{Ca,L}$ on intracellular EGTA (*triangles*) and BAPTA (*circles*). $I_{Ca,L}$ values were obtained after the maximal effects of BAPTA dialysis on $I_{Ca,L}$ had been reached, or after $I_{Ca,L}$ rundown during EGTA dialysis had plateaued after ~10 min. Open symbols represent averaged $I_{Ca,L}$ values recorded from cells preincubated and superfused with 10 μM ryanodine, and dialyzed with EGTA-containing (*triangles*) or BAPTA-containing (*circles*) solutions. Note that the open symbols at 0.2 mM buffer concentration are slightly moved to the right for visual clarity. Filled symbols are from control experiments without ryanodine treatment. The dependence of $I_{Ca,L}$ on intracellular BAPTA (0.2–50 mM) is fitted by a sigmoidal function. When cell dialysates contained BAPTA beyond 50 mM, many cells showed signs of losing striation and blebbing during the process of dialysis, usually accompanied by fast decay of $I_{Ca,L}$ before maximal stimulation was accomplished (see $I_{Ca,L}$ data corresponding to 60 mM BAPTA). This may suggest that a crucial level of Ca^{2+} underneath the membrane may be required to maintain the integrity of the lipid bilayer. Data are given as mean ± SEM, $n = 4$–19. Where error bars are absent, they are smaller than the size of the symbols.

is 5–7 μM with 40 mM EGTA. However, under the assumption that $i_{Ca,L}$ changes proportionally with $I_{Ca,L}$, Ca^{2+}_{sm} is lower with 0.2 mM EGTA than with 10 and 40 mM at ≤80 nm from the channel pore (Fig. 6 *Ba, left panel*) and Ca^{2+}_{sm} profiles in the presence of 10 and 40 mM BAPTA are not well separated (Fig. 6 *Bb, left panel*).

Is the superior buffering of Ca^{2+}_{sm} by BAPTA really required for the stimulation of $I_{Ca,L}$? To rule out other non-specific effects of BAPTA on $I_{Ca,L}$, we designed an intracellular solution that contains a mixture of 20 mM BAPTA and 20 mM dn-BAPTA (see Methods). Dn-BAPTA is an analog of BAPTA with a very low Ca^{2+} affinity ($K_D = 20$ mM, cf. Pethig et al., 1989). With respect to Ca^{2+}_i buffering, the Ca^{2+}_{sm} buffering power of the 20-mM BAPTA/20-mM dn-BAPTA mixture is similar to a 20-mM BAPTA solution, while the Ca^{2+}_c buffering of both solutions is sufficient (cf. Fig. 6 *Ab*). With respect to the total concentration of "BAPTA-like" ingredients, which could affect $I_{Ca,L}$ by chemical properties other than Ca^{2+} buffering, it resembles a 40-mM BAPTA dialysate. Fig. 7 *A* shows that 40 mM BAPTA stimulated $I_{Ca,L}$ by about fourfold, whereas the mixture of 20 mM BAPTA/20 mM dn-BAPTA could not even negate the rundown of $I_{Ca,L}$. As summarized in Fig. 7

B, the mixture of BAPTA and dn-BAPTA maintained an $I_{Ca,L}$ (5.56 ± 0.36 pA/pF, $n = 7$) which is significantly smaller ($p < 0.0001$) than that achieved with 40 mM BAPTA dialysis (34.9 ± 1.5 pA/pF, $n = 17$), but which is comparable ($p = 0.58$) to that achieved with 20 mM BAPTA alone (5.89 ± 0.43 pA/pF, $n = 9$). These data suggest that chemical properties of BAPTA other than Ca^{2+} buffering are unlikely to contribute significantly to the augmentation of $I_{Ca,L}$ described in this study.

Recently, Sipido et al. (1995) suggested an interaction between SR Ca^{2+} and sarcolemmal Ca^{2+} channels in guinea pig ventricular cardiomyocytes; thus, SR Ca^{2+} release may, to some extent, contribute to the Ca^{2+} gradient in the vicinity of the pore. To address this issue, we pretreated isolated cardiomyocytes with 10 μM ryanodine to block the release of SR Ca^{2+} (Marban and Wier, 1985). After the inhibition of SR Ca^{2+} release by ryanodine, the $I_{Ca,L}$ enhancement was still absent in either 0.2 mM EGTA (2.9 ± 0.4 pA/pF, $n = 2$) or 40 mM EGTA (4.2 ± 0.3 pA/pF, $n = 3$). Ryanodine treatment also had little effect on $I_{Ca,L}$ in 0.2 mM BAPTA (2.3 ± 0.1 pA/pF, $n = 3$) or 40 mM BAPTA (35.6 ± 1.2 pA/pF, $n = 4$) (also cf. Fig. 4). These results suggest that SR Ca^{2+} release does not contribute significantly to the Ca^{2+}_{sm} gradient that determines the amplitude of $I_{Ca,L}$ under our conditions.

Involvement of Ca^{2+}-sensitive adenylyl cyclase in the BAPTA-induced stimulation of $I_{Ca,L}$

Recent studies suggest that adenylyl cyclase regulation by factors other than G-proteins, particularly Ca^{2+}_i, may be an important modulator of enzyme activity and, thus, cAMP synthesis (e.g., Cooper et al., 1995; Sunahara et al., 1996). Moreover, there is indirect evidence that only Ca^{2+} entry, and not Ca^{2+} release, can regulate these enzymes (cf. Cooper et al., 1995). Because Ca^{2+}-inhibited adenylyl cyclase is the dominant isoform in cardiac tissue (e.g., Cooper et al., 1995), a lowering of Ca^{2+} within the vicinity of this membrane-bound enzyme would result in enhanced adenylyl cyclase activity, increased cAMP synthesis, and Ca^{2+} channel phosphorylation via PKA. Thus, we next investigated this possibility to account for BAPTA-induced stimulation of $I_{Ca,L}$.

At first, we ascertained whether BAPTA-elevated $I_{Ca,L}$ was still responsive to cAMP stimulation. Fig. 8 *Aa* shows that cell dialysis with 1 mM BAPTA did not affect $I_{Ca,L}$, and that subsequent bath application of 3 μM forskolin, a direct activator of adenylyl cyclase (Seamon and Daly, 1986), resulted in a 7.5-fold increase in $I_{Ca,L}$. In Fig. 8 *Ab*, after ≥600 s of cell dialysis with 50 mM BAPTA solution, $I_{Ca,L}$ was elevated by 4.1-fold and was largely insensitive to further stimulation by subsequent forskolin application. In contrast, cell dialysis with 50 mM EGTA did not stimulate $I_{Ca,L}$, and subsequent forskolin superfusion increased $I_{Ca,L}$ by 4.6-fold (Fig. 8 *B*). The similar $I_{Ca,L}$ increments in response to forskolin-induced cAMP elevation in cells dia-
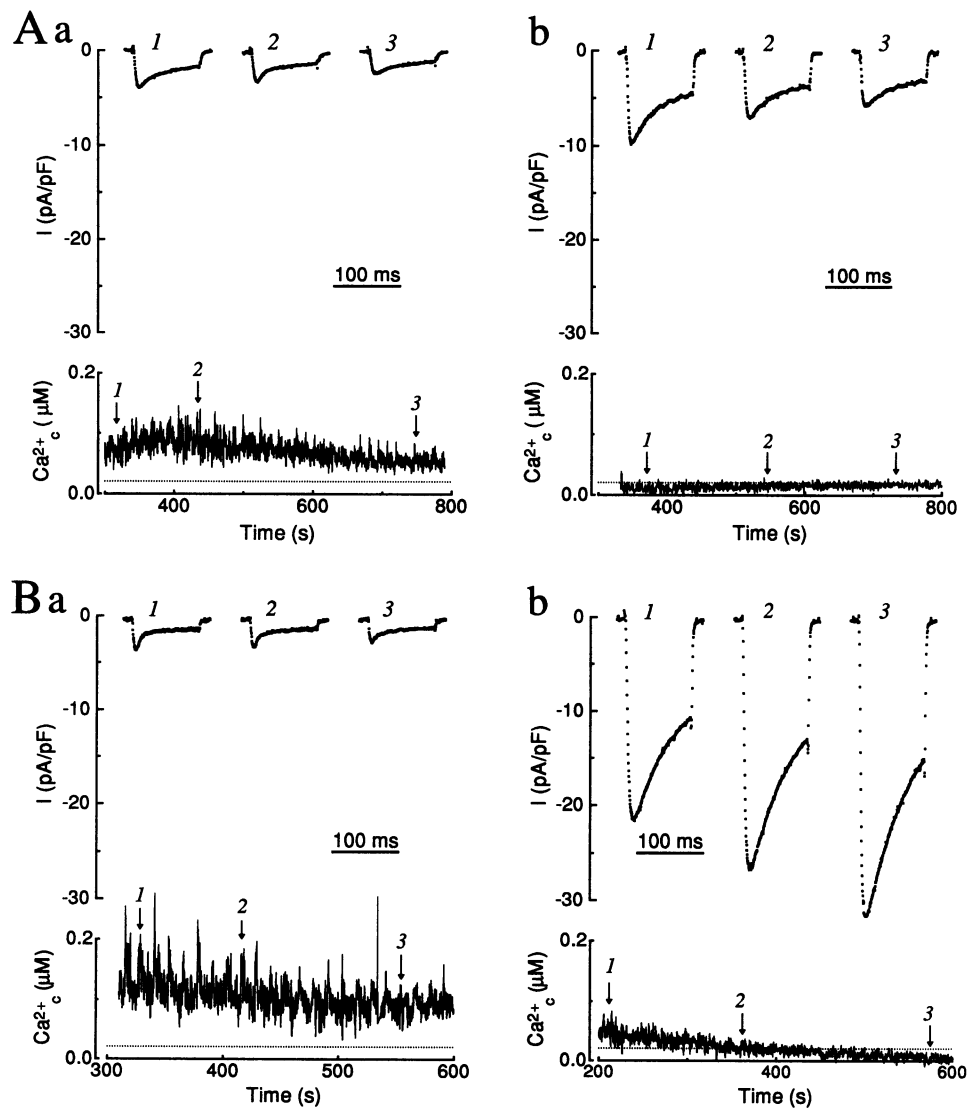
FIGURE 5 Simultaneous measurements of whole-cell $I_{Ca,L}$ and intracellular Ca^{2+} (Ca$_c^{2+}$) in myocytes dialyzed with intracellular solutions containing either EGTA (A) or BAPTA (B) as Ca^{2+} buffer. Four myocytes were dialyzed, respectively, with 0.2 mM EGTA (Aa), 40 mM EGTA (Ab), 0.2 mM BAPTA (Ba), and 40 mM BAPTA (Bb). In each panel, sample $I_{Ca,L}$ traces at three different times after patch breakthrough (1 to 3) were plotted along with the Ca$_c^{2+}$ value determined by indo-1. Dotted lines indicate the detection limit of indo-1 ($\sim$20 nM, see Methods). Arrows on top of Ca$_c^{2+}$ records indicate the times when the corresponding $I_{Ca,L}$ traces were recorded.

lyzed with low concentrations of BAPTA (Fig. 8 Aa) or high EGTA concentrations (Fig. 8 B) suggest that the buffering media do not affect the maximal $I_{Ca,L}$ response to cAMP (also see Fig. 9 A). An elevation of cAMP before BAPTA dialysis [(40 min preincubation of cells with 3 μM forskolin and 50 μM of the phosphodiesterase inhibitor IBMX (Fischmeister and Hartzell, 1990)] resulted in a post-patch $I_{Ca,L}$ (Fig. 8 C) comparable in size to (i) $I_{Ca,L}$ recorded after prolonged dialysis with 50 mM BAPTA (Fig. 8 Ab) and (ii) $I_{Ca,L}$ observed after 3 μM forskolin application to cells dialyzed with either 1 mM BAPTA (Fig. 8 Aa) or 50 mM EGTA (Fig. 8 B). $I_{Ca,L}$ in cAMP-upmodulated myocytes was not further increased by prolonged dialysis with 40 mM BAPTA solution (Fig. 8 C).

Fig. 9 A summarizes the dependence of $I_{Ca,L}$ sensitivity to forskolin stimulation of adenylyl cyclase on the concentration of intracellular Ca^{2+} chelator. The $I_{Ca,L}$-enhancing effect of internal BAPTA occluded that of forskolin (filled circles), with half-maximal inhibition of forskolin stimula-

tion at 26 mM BAPTA. In comparison, prolonged dialysis with EGTA up to 67 mM had a relatively small inhibitory effect on the potentiation of $I_{Ca,L}$ by forskolin (filled triangles). In addition, in cells dialyzed with the mixture of 20 mM BAPTA and 20 mM dn-BAPTA, the size of the $I_{Ca,L}$ increment induced by forskolin is similar to that in cells dialyzed with 20 mM BAPTA (open square). Cell dialysis with BAPTA and cAMP loading of myocytes resulted in identical $I_{Ca,L}$ densities (Fig. 9 B, $p > 0.5$) and both maneuvers rendered $I_{Ca,L}$ insensitive to subsequent forskolin-induced cAMP elevation and BAPTA dialysis, respectively (Fig. 9 B, $p > 0.5$ in all cases). These findings suggest that the augmentation of $I_{Ca,L}$ in response to BAPTA dialysis may be accounted for by an increase in myocyte cAMP levels via stimulation of adenylyl cyclase activity and subsequent activation of the cAMP cascade.

To further compare the similarities of $I_{Ca,L}$ stimulation by cAMP and by BAPTA, we next examined the kinetics of $I_{Ca,L}$ inactivation under the various experimental conditions
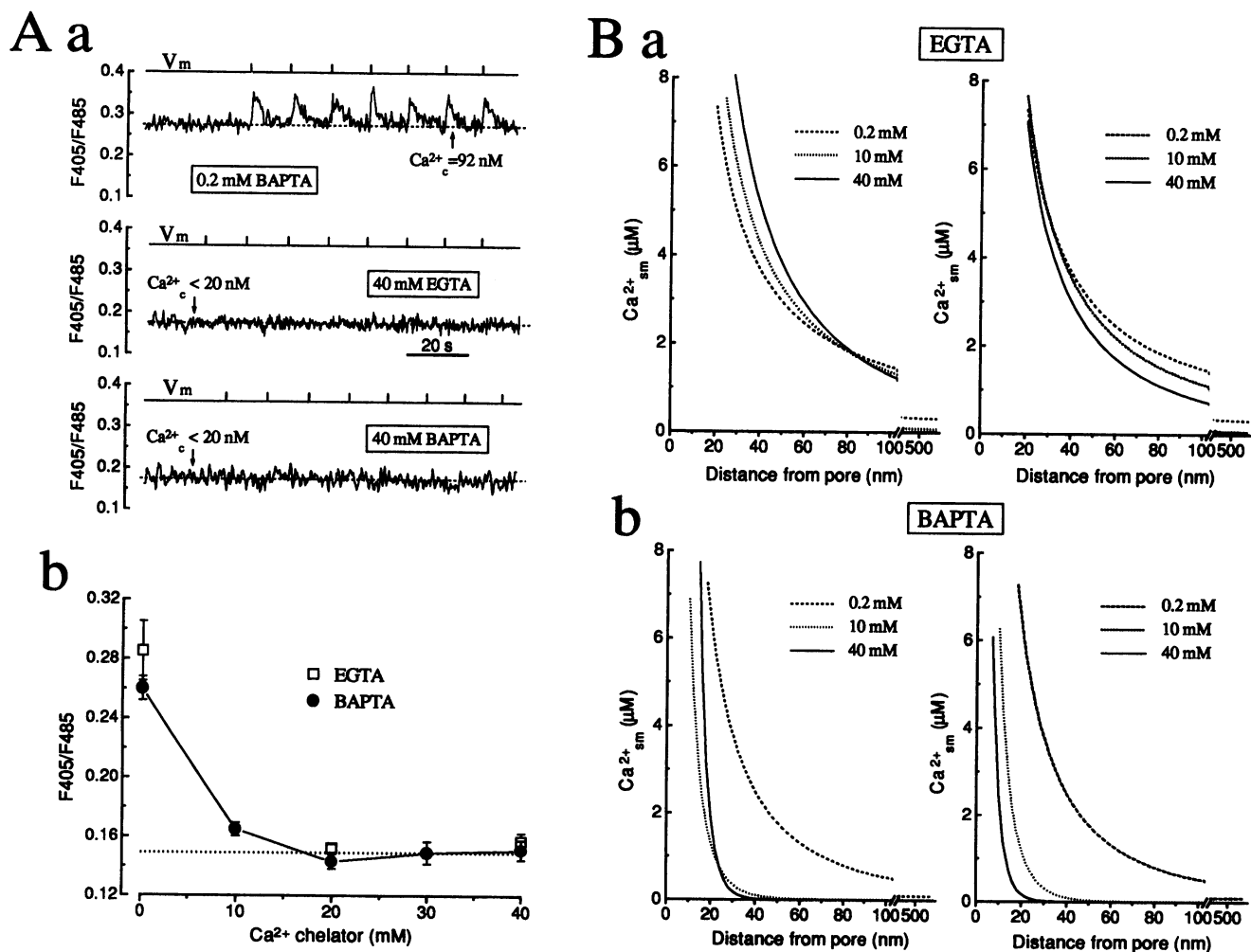
FIGURE 6 Buffering of bulk cytosolic Ca^{2+} (Ca_c^{2+}) and submembrane Ca^{2+} (Ca_{sm}^{2+}) by EGTA and by BAPTA. Panel Aa illustrates the Ca_c^{2+} changes in myocytes dialyzed with 0.2 mM EGTA and 40 mM of either EGTA or BAPTA. The Ca_c^{2+} level is expressed as the ratio of indo-1 fluorescence at 405 nm and 485 nm (F405/F485). V_m is the membrane potential, with each upward deflection representing a 100-ms depolarization from -40 mV to 0 mV. Dashed lines represent average indo-1 ratios in these quiescent myocytes; their corresponding Ca_c^{2+} values are given. Twenty nanomolar is regarded as the detection limit of indo-1 (see Methods). Panel Ab summarizes average fluorescence ratios in myocytes dialyzed with 0.2-40 mM EGTA (squares) or BAPTA (circles) ($n = 4-12$). The dotted line denotes R_{min} (see Methods). In panel B, the spatial distributions of Ca_{sm}^{2+} near the channel pore were derived according to Stern (1992)

$$Ca_{sm}^{2+} = [(Q_1 - Q_0) e^{-rW} + Q_0]/r + Ca_c^{2+}$$

where r is the distance from the pore, and Q_1, Q_0, and W are determined by the "on" and "off" rates of a Ca^{2+} chelator ($K_{on, BAPTA} = 9.4 \times 10^8$ M^{-1} s^{-1}, $K_{off, BAPTA} = 119$ s^{-1}, $K_{on, EGTA} = 1.5 \times 10^6$ M^{-1} s^{-1}, $K_{off, EGTA} = 0.22$ s^{-1}), by the diffusion coefficients of both chelators and the Ca^{2+} ion (1×10^9 m^2/s), by the total chelator concentration (2×10^{-4} to 0.04 M), and finally by the size of the current passing through the single Ca^{2+} channel ($i_{Ca,L}$). In our calculations, $i_{Ca,L}$ from cells dialyzed with 0.2 mM EGTA was assumed to be 0.2 pA in 1.8 mM external Ca^{2+} solution (cf. Rose et al., 1992 for 10 mM external Ca_o^{2+}). Unitary $i_{Ca,L}$ under other conditions was either scaled up according to its whole-cell $I_{Ca,L}$ amplitudes (left panels), or considered to be 0.2 pA regardless of the size of whole-cell $I_{Ca,L}$ (right panels). Refer to text for further discussions.

described in Fig. 8 (Table 1). When $I_{Ca,L}$ was stimulated by forskolin in myocytes dialyzed with ≥ 40 mM EGTA solutions (EGTA$_i$ → forskolin, Table 1), the slow time constant (τ_S) of $I_{Ca,L}$ inactivation decreased significantly, while the fast time constant (τ_F) remained constant (also cf. You et al., 1995). This is consistent with our previous findings (You et al., 1995) that τ_S is shortened by increases in Ca^{2+} flux through the channel, whereas τ_F is more sensitive to cyto-

solic Ca^{2+} changes, which in this case were well controlled. In myocytes dialyzed with ≥ 40 mM BAPTA solutions (BAPTA$_i$ → forskolin, Table 1), the τ_S value was comparable to forskolin-stimulated τ_S with ≥ 40 mM EGTA, but was significantly smaller than the EGTA control. Subsequent application of forskolin did not further change the value of τ_S. The τ_F values were unchanged under both conditions. In the last set of experiments (forskolin →
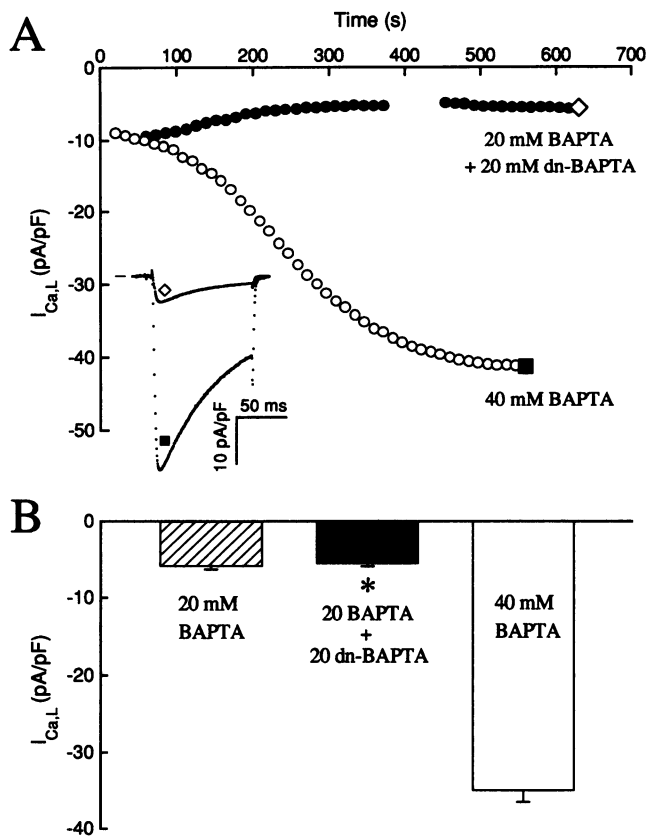
FIGURE 7 $I_{Ca,L}$ changes during cell dialysis with 40 mM BAPTA as compared to those obtained during dialysis with a mixture of 20 mM BAPTA/20 mM dn-BAPTA. (A) representative time courses of $I_{Ca,L}$ in two myocytes dialysis with 40 mM BAPTA (open circles) and 20 mM BAPTA/20 mM dn-BAPTA (filled circles), respectively. The inset shows two overlaid sample currents at the end of the respective time course. Average $I_{Ca,L}$ in 20 mM BAPTA/20 mM dn-BAPTA (n = 7) is shown in (B) along with $I_{Ca,L}$ averages from cells dialyzed with 20 mM BAPTA (n = 9) and with 40 mM BAPTA (n = 17). *, p = 0.58 compared with 20 mM BAPTA and p < 0.0001 compared with 40 mM BAPTA.

$BAPTA_i$), $I_{Ca,L}$ recorded in myocytes preincubated with forskolin and IBMX had τ_S values similar to those of forskolin-stimulated $I_{Ca,L}$ or those of BAPTA-stimulated $I_{Ca,L}$, whereas its τ_F value was significantly smaller, reflecting a higher Ca_c^{2+} before the dialysis of the Ca^{2+} chelator. Subsequent dialysis of BAPTA in these cells resulted in a doubling of τ_F. Finally, the relative magnitudes of fast inactivation $[A_F/(A_S + A_F)$; e.g., You et al., 1995] were more variable from cell to cell (e.g., 0.28 ± 0.10 with $EGTA_i$ + forskolin), but showed a general trend of declining with cell dialysis in all three experiments. These changes are partially attributable to a decrease in Ca_c^{2+} with time, especially in the last set of experiments. In summary, the kinetics of $I_{Ca,L}$ inactivation demonstrated good resemblance between forskolin-stimulated $I_{Ca,L}$ and BAPTA-stimulated $I_{Ca,L}$.

The gradual inhibition of forskolin stimulation with increasing $BAPTA_i$ as well as the occlusion of $BAPTA_i$ stimulation in cAMP-loaded cells suggest that Ca_{sm}^{2+} buff-

ering by BAPTA competes with forskolin in the activation of adenylyl cyclase and cAMP synthesis. If so, acetylcholine, which inhibits adenylyl cyclase and cAMP synthesis via an inhibitory G-protein (G_i) (Fleming et al., 1987) and thereby counteracts $I_{Ca,L}$ stimulation by forskolin in guinea pig ventricular myocytes (Hescheler et al., 1986), should antagonize BAPTA-induced stimulation of $I_{Ca,L}$. The example experiment in Fig. 10 Aa illustrates that 10 µM acetylcholine reversibly suppressed BAPTA-stimulated $I_{Ca,L}$. In five cells studied, acetylcholine (10 µM) attenuated 30-mM BAPTA-stimulated $I_{Ca,L}$ by 53.3 ± 1.6% (*, p = 0.002; Fig. 10 Ab). Acetylcholine (10 µM) had comparatively little effect on $I_{Ca,L}$ in five cells dialyzed with a 40-mM EGTA solution (**, p = 0.107; Fig. 10 Ab).

In a final series of experiments, we ascertained that BAPTA stimulation of $I_{Ca,L}$ resulted from PKA phosphorylation of Ca^{2+} channels. Bath application of 100 µM H-89, a competitive blocker of PKA (Yuan and Bers, 1995) partially reversed the augmentation of $I_{Ca,L}$ induced by cell dialysis with 30 mM BAPTA (Fig. 10 Ba). In six cells investigated, H-89 (100 µM) inhibited 30 mM BAPTA-stimulated $I_{Ca,L}$ by 43.8 ± 2.8% (*, p < 0.0001; Fig. 10 Bb).

DISCUSSION

The experiments described in this study demonstrate a novel effect of intracellular dialysis with high concentrations of BAPTA on L-type Ca^{2+} channel current in cardiomyocytes. Evidence provided here indicates that the $I_{Ca,L}$-enhancing effect of BAPTA is due to its fast Ca^{2+} buffering ability within macromolecular distances of the Ca^{2+} channel pore conducting picoampere Ca^{2+} current. Additional experimental data demonstrate a complete reciprocity of $I_{Ca,L}$ stimulation by BAPTA dialysis and by cAMP elevation with the adenylyl cyclase activator forskolin, and show the similarities in $I_{Ca,L}$ inactivation kinetics under these two conditions. Lastly, involvement of adenylyl cyclase and protein kinase A in the BAPTA-induced augmentation of $I_{Ca,L}$ is confirmed using interventions that suppress the enzymatic activities of these two important constituents in the cAMP signaling cascade.

The effects of Ca_{sm}^{2+} buffering by high BAPTA on $I_{Ca,L}$

Fig. 6 B demonstrates the superior buffering power of BAPTA, in comparison to EGTA, in the restricted diffusion space underneath the membrane near the Ca^{2+} conducting pore. The connection between Ca_{sm}^{2+} buffering by BAPTA and $I_{Ca,L}$ stimulation is strengthened by experiments using the inactive BAPTA analog dn-BAPTA. Although the qualitative differences between the degree of Ca_{sm}^{2+} buffering by EGTA and BAPTA are very clear at concentrations >10 mM (Fig. 6 B), no attempts are made to quantify the relation between $I_{Ca,L}$ and Ca_{sm}^{2+}. This is primarily due to the uncertainty of how to incorporate changes of whole-cell $I_{Ca,L}$ into

FIGURE 8   Effects of forskolin on $I_{Ca,L}$ after cell dialysis with BAPTA (*Aa*, 1 mM; *Ab*, 50 mM) or 50 mM EGTA (*B*), and effect of BAPTA dialysis on $I_{Ca,L}$ in cAMP-loaded cells (*C*). Three sample $I_{Ca,L}$ traces from each experiment are overlaid and labeled by the respective symbols shown in the time diaries of $I_{Ca,L}$ amplitude. The periods of 3 μM forskolin (*Fsk*) application are indicated by solid bars (*A*, *B*). Elevation of cAMP preceding Ca^{2+} buffering was achieved by preincubation of cells with 3 μM forskolin and 50 μM IBMX for 20–50 min before patch breakthrough and the onset of 40 mM BAPTA dialysis at time "0"; thereafter, the superfusate also contained 3 μM forskolin and 50 μM IBMX (*Fsk + IBMX, solid bar, C*). Note the slowing of $I_{Ca,L}$ inactivation after BAPTA dialysis in cAMP-loaded myocytes despite a lack of sizable effect on $I_{Ca,L}$ amplitude (also cf. Table 1).
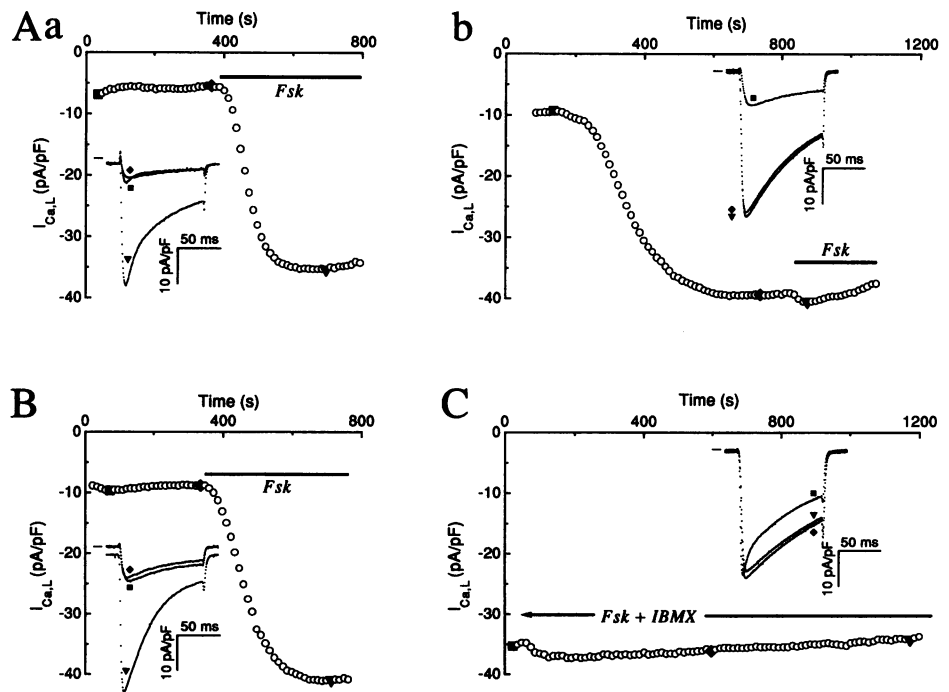
a model that is designed to calculate steady-state Ca_{sm}^{2+} profiles near a single Ca^{2+} channel conducting unitary $i_{Ca,L}$, but which does not account for changes in channel kinetics. It is likely that stimulation of $I_{Ca,L}$ under our experimental conditions results from increases in single-channel open probability and/or availability rather than an augmentation in elementary current amplitude (cf. McDonald et al., 1994). However, if we consider a contribution of Ca^{2+} from adjacent open channels to the Ca_{sm}^{2+} profile established by any individual channel (e.g., Imredy and Yue, 1992), the most conservative approach (which will likely overestimate Ca_{sm}^{2+} with large $I_{Ca,L}$) is to model the increases in whole-cell $I_{Ca,L}$ as proportional increases in single-channel Ca^{2+} conductance (Fig. 6 *B, left panels*). On the other hand, if we assume that the cross talk between adjacent channels can be eliminated with even submillimolar BAPTA (Imredy and Yue, 1992), then Ca^{2+} influx used in the theoretical model can be considered to be independent of the size of $I_{Ca,L}$ (Fig. 6 *B, right panels*). In addition to the difficulties with incorporating $I_{Ca,L}$ amplitude into Ca_{sm}^{2+} calculations, some inherent limitations of the model may also compromise an accurate representation of the whole-cell situation. For example, contribution of a potential diffusional barrier (such as sarcoplasmic reticulum) is not considered (cf. Kargacin, 1994). Such a barrier may limit the effective BAPTA concentration in the close proximity of the channel, as well as hinder the diffusion of Ca_{sm}^{2+} to the center of the cytoplasm. In summary, although theoretical computation provides important insights regarding Ca_{sm}^{2+} buffering by EGTA and BAPTA, it seems premature to interpret the results in quantitative terms. Experiments using lipophilic Ca^{2+} indicators such as fura-C_{18} and fura-indoline-C_{18} and/or confocal laser scan-

ning microscopy may ultimately provide more accurate estimates of Ca_{sm}^{2+} and its relation to $I_{Ca,L}$.

In the following, we discuss some possible mechanisms by which reducing Ca_{sm}^{2+} may have led to the large augmentation of $I_{Ca,L}$ observed in this study. The first possible
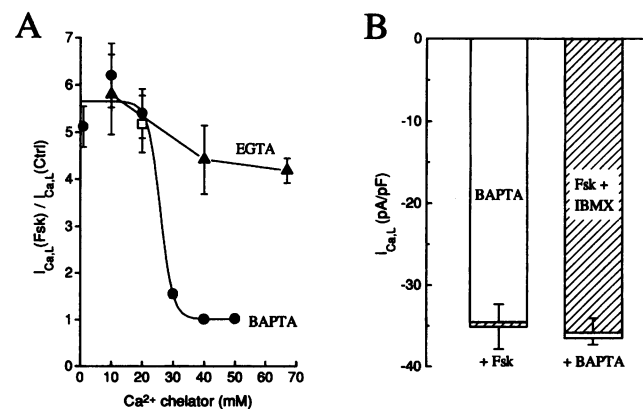
FIGURE 9   Dependence of $I_{Ca,L}$ stimulation by forskolin on intracellular EGTA or BAPTA concentrations (*A*) as well as the effect of BAPTA dialysis in cAMP-loaded cells (*B*). In panel *A*, the degree of $I_{Ca,L}$ stimulation by forskolin is expressed as the ratio of forskolin-stimulated $I_{Ca,L}$ over control $I_{Ca,L}$ just before forskolin application [$I_{Ca,L}$(Fsk)/$I_{Ca,L}$(Ctrl)]. $n = 3$–24 (expect for 50 mM BAPTA, where $n = 2$). The open square represents the degree of forskolin stimulation in seven cells dialyzed with a 20-mM dn-BAPTA/20-mM BAPTA mixture. In panel *B*, $I_{Ca,L}$ from five cells dialyzed with 40 mM BAPTA (*BAPTA*) and subsequently exposed to 3 μM forskolin (*+Fsk*) are contrasted with those from five cells preincubated and superfused with 3 μM forskolin and 50 μM IBMX (*Fsk + IBMX*) and subsequently dialyzed with 40 mM BAPTA for $\geq$15 min (*+BAPTA*).

TABLE 1 Effects of EGTA, BAPTA, and forskolin on the kinetics of $I_{Ca,L}$ inactivation

Protocols*	EGTA$_i$ → forskolin		BAPTA$_i$ → forskolin		forskolin → BAPTA$_i$	
Conditions#	EGTA$_i$	+forskolin	BAPTA$_i$	+forskolin	forskolin/IBMX	BAPTA$_i$
τ_s (ms)	173 ± 6 (17)	125 ± 9§ (5)	127 ± 4 (17)	135 ± 6 (6)	127 ± 2 (4)	138 ± 4¶ (4)
τ_F (ms)	19.1 ± 0.7 (17)	19.2 ± 0.8§ (5)	19.8 ± 0.8 (17)	21.7 ± 0.6 (6)	11.3 ± 0.8 (4)	23.7 ± 1.0§ (4)
$A_F/(A_F + A_S)$	0.33 ± 0.02 (17)	0.28 ± 0.10 (5)	0.31 ± 0.04 (17)	0.14 ± 0.02§ (6)	0.35 ± 0.01 (4)	0.10 ± 0.04§ (4)

All values are expressed as mean ± SEM, followed by numbers of measurements in the parentheses.
* Refer to legend of Fig. 8 and text for detailed description of experimental protocols.
EGTA$_i$, cell dialysis with 40, 50, and 67 mM EGTA solution; BAPTA$_i$, dialysis with 40 and 50 mM BAPTA.
§ $p < 0.05$ compared with values in previous column.
¶ $p = 0.049$ compared with the value in previous column—marginally significant.

scenario is that reduction in Ca_{sm}^{2+} increases the Ca^{2+} driving force across the cell membrane, thus resulting in larger $I_{Ca,L}$. This hypothesis is faced with the following three difficulties. (i) Bath application of acetylcholine or H-89 reversibly inhibited the BAPTA-stimulated $I_{Ca,L}$ (Fig. 10). This is inconsistent with the Ca^{2+} driving force theory because Ca_{sm}^{2+} buffering by BAPTA was not likely compromised under these conditions. Contrarily, the driving force is expected to increase because the reduction of Ca^{2+} influx may lower Ca_{sm}^{2+}. (ii) According to the calculation illustrated in Fig. 6 B, Ca_{sm}^{2+} reduction by BAPTA is limited at a distance of ≥20 nm from the pore, whereas at shorter distances, BAPTA becomes as ineffective as EGTA in achieving good control of Ca_{sm}^{2+}. In fact, even for an "ideal chelator" with an infinite rate of Ca^{2+} buffering, the model by Stern (1992) predicts that diffusion will limit efficient Ca^{2+} buffering at <1 nm. Thus, the effective Ca^{2+} gradient across the channel is not expected to be steeper in myocytes dialyzed with high concentrations of BAPTA. On the contrary, inasmuch as $I_{Ca,L}$ was enhanced severalfold with high BAPTA, the increased Ca^{2+} influx might actually elevate Ca_{sm}^{2+} in the immediate vicinity of the channel pore, thus reducing the driving force. (iii) The amplitude of unitary $i_{Ca,L}$ is proportional to the Ca^{2+} driving force across the membrane only if the open Ca^{2+} channel resembles a water-filled pore, through which Ca^{2+} diffuses freely down its electrochemical gradient. In reality, however, Ca^{2+} permeation is likely in a single-file fashion, and involves binding of Ca^{2+} to multiple sites within the conductive pore (Hess and Tsien, 1984). Thus, the relation between $i_{Ca,L}$ and Ca^{2+} driving force may be more complicated. In fact, while increasing external Ca^{2+} from 1 to ~40 mM leads to progressively larger single-channel conductance (cf. McDonald et al., 1994), elevation of internal Ca^{2+} has little influence on the amplitude of $i_{Ca,L}$. For example, Imredy and Yue (1994) have shown that when cells were loaded with Ca^{2+} by means of conditioning prepulses, subsequently elicited single-channel $i_{Ca,L}$ was similar in amplitude compared to controls. When L-type Ca^{2+} channels were incorporated in planar lipid bilayers, the amplitude of unitary $i_{Ca,L}$ was insensitive to changes in internal Ca^{2+} from 20 nM to 15 μM (Haack and Rosenberg, 1994). Taken together, it seems unlikely that changes in Ca^{2+} driving force play a significant role in the BAPTA-induced stimulation of $I_{Ca,L}$ reported here.

Secondly, single-channel studies by Imredy and Yue (1994) and by Haack and Rosenberg (1994) indicate that elevation of Ca^{2+} on the cytoplasmic side of the Ca^{2+} channel decreases its open probability, thus reducing the ensemble average Ca^{2+} current. We have recently suggested that Ca^{2+}-dependent inactivation may reduce the amplitude of whole-cell $I_{Ca,L}$ by inactivating Ca^{2+} channels
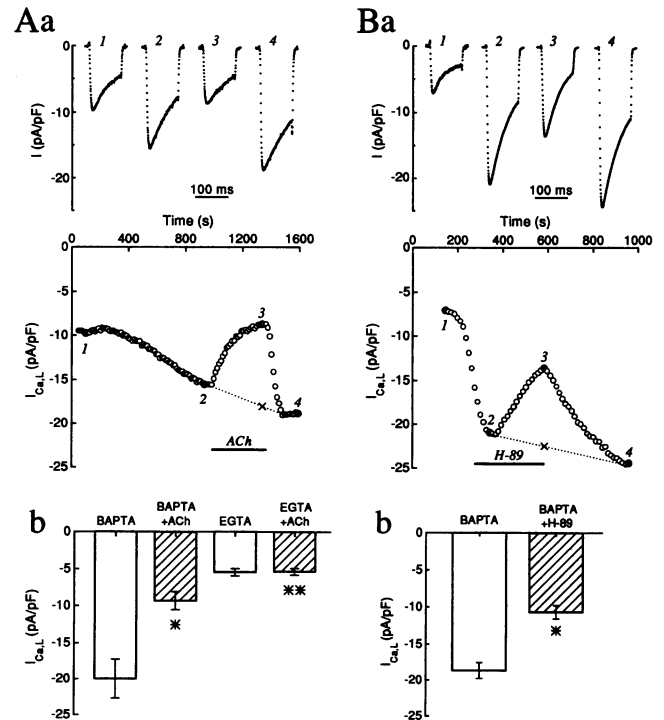
FIGURE 10 Reversible inhibition of BAPTA-stimulated $I_{Ca,L}$ by acetylcholine (A, ACh) and by H-89 (B). Cell dialysates contained 30 mM BAPTA (A, B) or 40 mM EGTA (Ab). Sample $I_{Ca,L}$ traces before, during, and after bath application of 10 μM acetylcholine (A) and 100 μM H-89 (B) are shown in the top panels. The center panels illustrate time courses of $I_{Ca,L}$ in response to BAPTA dialysis and subsequent acetylcholine (A) or H-89 (B) superfusion; the latter is indicated by solid bars (Ach, H-89). The overshoot of $I_{Ca,L}$ after acetylcholine and H-89 withdrawal is likely due to continued BAPTA dialysis during the period of drug superfusion. Panels b summarize average $I_{Ca,L}$ values (mean ± SEM, $n = 5$ for acetylcholine, $n = 6$ for H-89) after 10 to 15 min of BAPTA (or EGTA, $n = 5$) dialysis (at x, obtained from the extrapolations shown as dotted lines in the center panels), and after acetylcholine or H-89 superfusion (BAPTA + ACh, EGTA + ACh, BAPTA + H-89, corresponding to solid symbol 3 in the time courses). * and ** represent p values given in text.
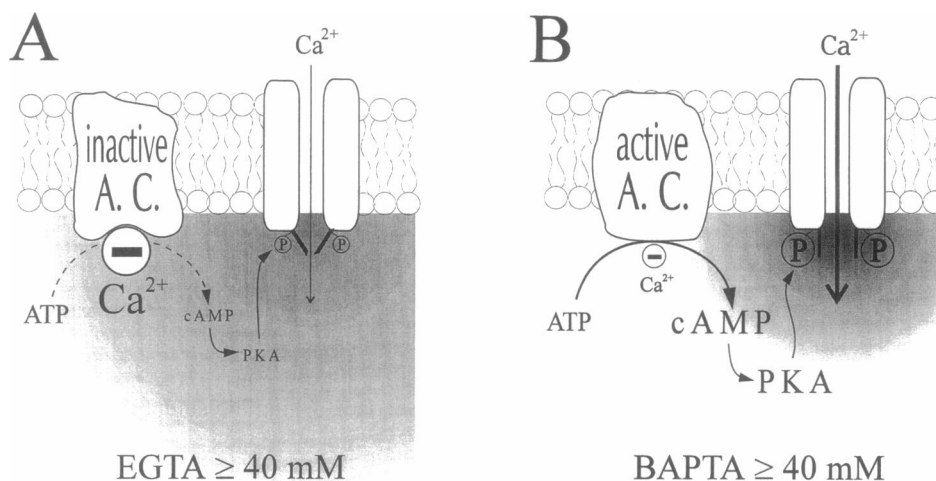
FIGURE 11   Proposed model of the Ca_{sm}^{2+} regulation of the cAMP cascade via a Ca^{2+}-sensitive adenylyl cyclase. Panel A represents a situation when cells are loaded with 40 mM EGTA. Ca^{2+} entry creates a high Ca_{sm}^{2+} region underneath the cell membrane, which inhibits adenylyl cyclase activity ("inactive A.C."). The reduction of cAMP synthesis eventually decreases channel phosphorylation and restricts Ca^{2+} influx. Such a negative feedback loop could potentially generate out-of-phase Ca^{2+} and cAMP oscillations in the restricted diffusion space underneath the membrane (cf. Cooper et al., 1995). In the presence of 40 mM BAPTA (B), the radius of the high Ca_{sm}^{2+} region is smaller, despite a potentially higher Ca_{sm}^{2+} in the immediate vicinity of the channel pore (due to the increase in Ca^{2+} entry). Low Ca_{sm}^{2+} around the adenylyl cyclase disinhibits its enzymatic activity, leading to robust Ca^{2+} channel phosphorylation and stimulation of $I_{Ca,L}$.

before channel opening is complete, and that the inactivation of $I_{Ca,L}$ depends on both cytoplasmic Ca^{2+} and Ca^{2+} in the restricted diffusion space underneath the membrane (You et al., 1995). This raises the possibility that, due to the buffering of Ca_{sm}^{2+}, BAPTA slows $I_{Ca,L}$ inactivation and thus augments $I_{Ca,L}$ amplitude. However, results in Table 1 argue against this hypothesis. When we compare $I_{Ca,L}$ inactivation kinetics in myocytes after prolonged dialysis with EGTA ($EGTA_i$, 2nd column) and BAPTA ($BAPTA_i$, 4th column), we find that parameters regarding the fast inactivation process, namely τ_F and $A_F/(A_F + A_S)$, are not significantly different. This is probably because, as we proposed previously (You et al., 1995), the fast inactivation predominantly depends on bulk Ca_c^{2+}, which is equally well controlled by EGTA and by BAPTA (apparent K_D for EGTA and BAPTA are 149 nM and 127 nM, respectively). Because only the fast inactivation process significantly reduces $I_{Ca,L}$ amplitude ($\tau_F \approx$ activation time or time-to-peak), cell dialysis with BAPTA is not likely to add favorably to the large augmentation of $I_{Ca,L}$ by attenuating $I_{Ca,L}$ inactivation. It is worth noting that the doubling of $I_{Ca,L}$ with increasing EGTA concentration from 0.2 to 67 mM may reflect the relief of Ca_c^{2+}-induced inhibition of $I_{Ca,L}$ observed by us (You et al., 1994) and by others (cf. McDonald et al., 1994).

Finally, it has been shown that reducing intracellular Mg^{2+} <1 mM results in substantial potentiation of $I_{Ca,L}$ (White and Hartzell, 1988; Agus et al., 1989; La and Pelzer, unpublished results). However, the possibility that high BAPTA augments $I_{Ca,L}$ by reducing Mg_i^{2+} is easily rejected because the Mg^{2+} chelating power of BAPTA is exactly identical to that of EGTA (apparent K_D = 20 mM at pH 7.2 for both Ca^{2+} chelators).

Possible role of a Ca^{2+}-sensitive adenylyl cyclase

The experimental evidence presented here indicates that lowering of peri-channel Ca^{2+} stimulates cAMP synthesis and channel phosphorylation via PKA by disinhibiting a Ca^{2+}-sensitive adenylyl cyclase, most likely the type VI isoform, which is expressed predominantly in heart (cf. Cooper et al., 1995; Sunahara et al., 1996). A dominant role for an inhibition of Ca^{2+}-dependent phosphatase(s) by BAPTA dialysis seems unlikely, as BAPTA was unable to augment peak $I_{Ca,L}$ in cAMP-loaded cells, where Ca_c^{2+} was seemingly high before cell dialysis with the Ca^{2+} chelator (Fig. 8 C, Table 1). Analogous to our conclusion, a recent biochemical study on chick heart cells and membranes indicated that submicromolar Ca^{2+} concentrations directly inhibited adenylyl cyclase activity and that the cAMP-elevating effects of isoprenaline and forskolin were increased as extracellular Ca^{2+} was lowered, an effect antagonized by the Ca^{2+} channel agonist BAY K 8644 (Yu et al., 1993). Similarly, the Ca^{2+} channel blockers D-600 and nifedipine potentiated the cAMP-elevating effect of isoprenaline in the presence of extracellular Ca^{2+} (Yu et al., 1993).

Fig. 11 illustrates our proposed model describing how Ca^{2+}-sensitive adenylyl cyclase intertwines cellular signaling by Ca^{2+} and cAMP. Fig. 11 A shows that high peri-channel Ca^{2+} in the presence of EGTA suppresses the enzymatic activity of nearby the adenylyl cyclase ("A.C."), probably via an intermediate, because no Ca^{2+} binding motif has been identified in the sequences of Ca^{2+}-inhibited adenylyl cyclases (e.g., Cooper et al., 1995). Ca^{2+} inhibition of adenylyl cyclase activity reduces the synthesis of cAMP, which in turn attenuates Ca^{2+} channel phosphorylation by PKA. Ca^{2+} influx through the L-type Ca^{2+} chan-

nel is restricted. In the presence of high BAPTA (Fig. 11 B), lowering of Ca^{2+} within macromolecular distances of the Ca^{2+} channel pore disinhibits adenylyl cyclase activity, leading to increased cAMP synthesis and channel phosphorylation by PKA. As a result, Ca^{2+} influx through the L-type Ca^{2+} channel is augmented.

Results from this study also indicate that Ca^{2+}-sensitive adenylyl cyclase is largely unaffected by bulk Ca_c^{2+}; efficient buffering of Ca_c^{2+} below 20 nM by intracellular EGTA $\geq$40 mM largely failed to potentiate $I_{Ca,L}$ with time (Fig. 1 A). Ca^{2+} release from the sarcoplasmic reticulum also seems ineffective in inhibiting adenylyl cyclase, since block of Ca^{2+} release from the sarcoplasmic reticulum by 10 μM ryanodine had little effect on $I_{Ca,L}$ in cells dialyzed with either EGTA or BAPTA at low and high concentrations (cf. open symbols in Fig. 4). Thus, it is the Ca^{2+} close to L-type Ca^{2+} channel entry sites that seems to be responsible for the modulation of Ca^{2+}-sensitive adenylyl cyclase activity.

REFERENCES

Agus, Z. S., E. Kelepouris, I. Dukes, and M. Morad. 1989. Cytosolic magnesium modulates calcium channel activity in mammalian ventricular cells. Am. J. Physiol. 256:C452–C455.

Cooper, D. M. F., N. Mons, and J. W. Karpen. 1995. Adenylyl cyclases and the interaction between calcium and cAMP signalling. Nature (Lond.). 374:421–424.

Fischmeister, R., and H. C. Hartzell. 1990. Regulation of calcium current by low-Kₘ cyclic AMP phosphodiesterases in cardiac cells. Mol. Pharmacol. 38:426–433.

Fleming, J. W., R. A. Strawbridge, and A. M. Watanabe. 1987. Muscarinic receptor regulation of cardiac adenylate cyclase activity. J. Mol. Cell. Cardiol. 19:47–61.

Grynkiewicz, G., M. Poenie, and R. Y. Tsien. 1985. A new generation of Ca²⁺ indicators with greatly improved fluorescence properties. J. Biol. Chem. 260:3440–3450.

Gurney, A. M., P. Charnet, J. M. Pye, and J. Nargeot. 1989. Augmentation of cardiac calcium current by flash photolysis of intracellular caged-Ca²⁺ molecules. Nature (Lond.). 341:65–68.

Haack, J. A., and R. L. Rosenberg. 1994. Calcium-dependent inactivation of L-type calcium channels in planar lipid bilayers. Biophys. J. 66: 1051–1060.

Hadley, R. W., and W. J. Lederer. 1991. Ca²⁺ and voltage inactivate Ca²⁺ channels in guinea-pig ventricular myocytes through independent mechanisms. J. Physiol. 444:257–268.

Hamill, O. P., A. Marty, E. Neher, B. Sakmann, and F. J. Sigworth. 1981. Improved patch-clamp techniques for high-resolution current recording from cells and cell-free membrane patches. Pfluegers Arch. 391:85–100.

Hescheler, J., M. Kameyama, and W. Trautwein. 1986. On the mechanism of muscarinic inhibition of the cardiac Ca current. Pfluegers Arch. 407:182–189.

Hess, P., and R. W. Tsien. 1984. Mechanism of ion permeation through calcium channels. Nature (Lond.). 309:453–456.

Hirano, Y., and M. Hiraoka. 1994. Dual modulation of unitary L-type Ca²⁺ channel currents by [Ca²⁺]ᵢ in fura-2-loaded guinea-pig ventricular myocytes. J. Physiol. 480.3:449–463.

Imredy, J. P., and D. T. Yue. 1992. Submicroscopic Ca²⁺ diffusion mediates inhibitory coupling between individual Ca²⁺ channels. Neuron. 9:197–207.

Imredy, J. P., and D. T. Yue. 1994. Mechanism of Ca²⁺-sensitive inactivation of L-type Ca²⁺ channels. Neuron. 12:1301–1318.

Kargacin, G. J. 1994. Calcium signaling in restricted diffusion spaces. Biophys. J. 67:262–272.

Kargacin, G. J., and F. S. Fay. 1991. Ca²⁺ movement in smooth muscle cells studied with one- and two-dimensional diffusion models. Biophys. J. 60:1088–1100.

Kokubun, S., and H. Irisawa. 1984. Effects of various intracellular Ca ion concentrations on the calcium current of guinea-pig single ventricular cells. Jpn. J. Physiol. 34:599–611.

Lattanzio, F. A., and D. K. Bartschat. 1991. The effect of pH on rate constants, ion selectivity and thermodynamic properties of fluorescent calcium and magnesium indicators. Biochem. Biophys. Res. Commun. 177:184–191.

Leblanc, N., and J. R. Hume. 1990. Sodium current-induced release of calcium from cardiac sarcoplasmic reticulum. Science. 248:372–376.

Lederer, W. J., E. Niggli, and R. W. Hadley. 1990. Sodium-calcium exchange in excitable cells: fuzzy space. Science. 248:283.

Marban, E., and W. G. Wier. 1985. Ryanodine as a tool to determine the contributions of calcium entry and calcium release to the calcium transient and contraction of cardiac Purkinje fibers. Circ. Res. 56:133–138.

McDonald, T. F., S. Pelzer, W. Trautwein, and D. J. Pelzer. 1994. Regulation and modulation of calcium channels in cardiac, skeletal, and smooth muscle cells. Physiol. Rev. 74:365–507.

Neher, E. 1986. Concentration profiles of intracellular calcium in the presence of a diffusible chelator. Exp. Brain Res. 14:80–96.

Pethig, R., M. Kuhn, R. Payne, E. Adler, T.-H. Chen, and L. F. Jaffe. 1989. On the dissociation constants of BAPTA-type calcium buffers. Cell Calcium. 10:491–498.

Pusch, M., and E. Neher. 1988. Rates of diffusional exchange between small cells and a measuring patch pipette. Pfluegers Arch. 411:204–211.

Rose, W. C., C. W. Balke, W. G. Wier, and E. Marban. 1992. Macroscopic and unitary properties of physiological ion flux through L-type Ca²⁺ channels in guinea-pig heart cells. J. Physiol. 456:267–284.

Seamon, K. B., and J. W. Daly. 1986. Forskolin: its biological and chemical properties. Adv. Cyclic Nucleotide Protein Phosphorylation Res. 20:1–150.

Sipido, K. R., G. Callewaert, and E. Carmeliet. 1995. Inhibition and rapid recovery of Ca²⁺ current during Ca²⁺ release from sarcoplasmic reticulum in guinea pig ventricular myocytes. Circ. Res. 76:102–109.

Smith, S. J., and G. J. Augustine. 1988. Calcium ions, active zones and synaptic transmitter release. TINS. 11:458–464.

Smith, P. D., G. W. Liesegang, R. L. Berger, G. Czerlinski, and R. J. Podolshy. 1984. A stopped-flow investigation of calcium ion binding by ethylene glycol bis(beta-aminoethylether)-N, N'-tetraacetic acid. Anal. Biochem. 143:188–195.

Stern, M. D. 1992. Buffering of calcium in the vicinity of a channel pore. Cell Calcium. 13:183–192.

Sunahara, R. K., C. W. Dessauer, and A. G. Gilman. 1996. Complexity and diversity of mammalian adenylyl cyclases. Annu. Rev. Pharmacol. Toxicol. 36:461–480.

Tseng, G.-N., and P. A. Boyden. 1991. Different effects of intracellular Ca and protein kinase C on the cardiac T and L Ca currents. Am. J. Physiol. 261:H364–H379.

White, R. E., and H. C. Hartzell. 1988. Effects of intracellular free magnesium on calcium current in isolated cardiac myocytes. Science. 239:778–780.

You, Y., D. J. Pelzer, and S. Pelzer. 1994. Modulation of calcium current density by intracellular calcium in isolated guinea pig ventricular cardiomyocytes. Biochem. Biophys. Res. Commun. 204:732–740.

You, Y., D. J. Pelzer, and S. Pelzer. 1995. Trypsin and forskolin decrease the sensitivity of L-type calcium current to inhibition by cytoplasmic free calcium in guinea pig heart muscle cells. Biophys. J. 69:1838–1846.

Yu, H. J., H. Ma, and R. D. Green. 1993. Calcium entry via L-type calcium channels acts as a negative regulator of adenylyl cyclase activity and cyclic AMP levels in cardiac myocytes. Mol. Pharmacol. 44:689–693.

Yuan, W., and D. M. Bers. 1995. Protein kinase inhibitor H-89 reverses forskolin stimulation of cardiac L-type calcium current. Am. J. Physiol. 268:C651–C659.